VISCOSITY AND DENSITY

OF

REFERENCE FLUID

A thesis

submitted in partial fulfilment

of the requirements for the Degree

of

Master of Science in Physics

by

Masaed Moti Almotari

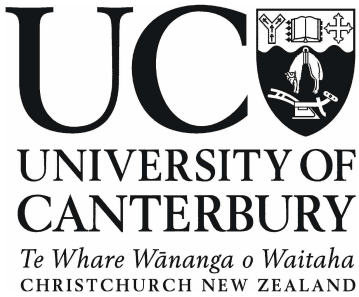

University of Canterbury

2006

Abstract

The viscosity and density of bis(8-methylnonyl) benzene-1,2-dicarboxylate {diisodecyl phthalate (DIDP)}, with a nominal viscosity at $T = 298$ K and $p = 0.1$ MPa of 87 mPa·s, have been measured at temperatures from (298.15 to 423.15) K and pressures from (0.1 to 70) MPa. A vibrating wire viscometer, with a wire diameter of about 0.15 mm, was utilised for the viscosity measurements and the results have an expanded uncertainty, ($k = 2$), including the error arising from the pressure measurement, of between ±(2 and 2.5) % The density was determined with two vibrating tube densimeters one for operation at $p \approx 0.1$ MPa with an expanded uncertainty ($k = 2$) of about ±0.1 %, the other that used at pressures up to 70 MPa, with an estimated expanded uncertainty ($k = 2$) of about ±0.3 %. Measurements of density and viscosity were performed on three samples of DIDP each with different purity stated by the supplier and as a function of water mass fraction. The measured viscosity and density are represented by interpolating expressions with differences between the experimental and calculated values that are comparable with the

expanded ($k = 2$) uncertainties. The obtained viscosities at $p = 0.1$ MPa agree with values reported in the literature within the combined expanded ($k = 2$) uncertainties of the measurements while our densities differ by no more than 1.5 %. Viscosity data at $p > 0.1$ MPa deviate systematically from the literature values in the range of -10 % to 10 %.

An apparatus capable of simultaneously measuring the solubility of a gas dissolved in a liquid and the viscosity and the density of the resulting mixture over a wide temperature and pressure range was constructed and tested. Preliminary results have been reported.

Acknowledgements

I would like to express my sincere thank to my supervisor Professor Ken Marsh, from the Chemical and Engineering Department, for his guidance and invaluable encouragement. He has kindly offered me this project. I am fortunate to be able to work with someone like him who has spent most of his life working in many scientific areas. In reality, working with him was a turning point in my life.

I am deeply indebted to my supervisor Dr. Roger Reeves, from the Physics and Astronomy Department, for allowing and supporting me to carry out this project.

I am very grateful to Dr. Mohammed Kandil for his endless assistance, instructive discussion, invaluable advice and his personal and moral support.

I should acknowledge all the help that I have received from a number of people, particularly Mr. Bob Gordon, Mr. Peter Jones, Mr. Trevor Berry and Mr. David Brown.

Finally, I would like to thank my parents, my brothers and my wife for their open-handed support and love.

TABLE OF CONTENTS

Chapter 4: Theory and Calculation Procedure

Chapter 5: Experimental consideration

CHAPTER 6: RESULTS AND DISCUSSION

CHAPTER 7: SOLUBILITY MEASUREMENT

LIST OF FIGURES:

LIST OF TABLES:

Chapter 1

GENERAL INTRODUCTION

1.1 Thesis layout:

This thesis is divided into six chapters as follows: Chapter One provides general and essential scientific information associated with viscosity, including its significance and the research motivations. Chapter Two gives an overview of various techniques to measure viscosity that have been developed, and their advantages and disadvantages. The next three chapters are devoted to discussing the main part of this work, the vibrating wire viscometer. This includes a literature review of the fluid sample used and other experimental devices involved. Chapter Six is allotted to the results and discussion. Finally, the design and construction of solubility apparatus and its initial test were discussed in Chapter Seven.

1.2 Study Motivation:

The variety of viscometers that are used for performing accredited viscosity measurements or for the establishment of a viscosity scale must be referable to the viscosity of the sole international primary standard[1]. Although the International Association Transport

Properties (previously known as the subcommittee on Transport Properties of The International Union of Pure and Applied Chemistry (IUPAC)) has made attempts to examine other recommended fluids for viscosity standards, the viscosity of water at 20 ^{o}C and at atmospheric pressure, (1.002 ± 0.0025) mPa·s, is still the only internationally accepted value[2]. In order to make viscosity measurements on more viscous fluids typically found in industrial applications, or to calibrate a viscometer at high pressure, additional working reference fluids with higher viscosities are used. The viscosity of these reference fluids are determined by the so-called "step-up" procedure using a series of master capillary viscometers, along overlapping ranges, starting with water as the reference fluid[1]. The measurements are made in National Standards Laboratories or other certified laboratories around the world and result in a set of certified fluids. Every sequential step in this procedure is associated with an uncertainty and this uncertainty is propagated with the increase with the number of comparisons. In addition, these reference fluids have limited shelf life because they are complex mixtures which oxidize and change composition with time[1]. Hence, there has been a search for some time for reference fluids that are pure fluids and can be purchased from normal

chemical suppliers. In addition, there are considerable labour and monetary costs in calibrating the present reference fluids and the validating procedure. The Bureau International des Poids et Measures (BIPM) has increasingly realized the need for such a standard. Thus IUPAC has been in charge of a project named "Investigation of a New High-Viscosity Standard''[3]. Diisodecyl Phthalate (DIDP) has been proposed as a suitable candidate in the range (100 to 200 mPa·s) because of its suitable characteristics such as high viscosity, an extended liquid-phase over a wide range of temperatures, availability, low volatility and non-toxicity[3]. The purpose of this work is to provide reference quality data on the DIDP viscosity and density and compare the results with other measurements that have been made in order to make a decision on its adequacy.

There are numerous techniques for measuring viscosity. One method, the vibrating wire, has been used in this work to measure the viscosity of DIDP because such a device can be operated over a wide range of temperatures and pressures[4,5]. Measurements are needed from (298 to 423) K and pressures from (0.1 to 70) MPa, which should go part way to satisfying industrial requirements. The theory of the vibrating wire requires knowledge of the density of

the fluid, so two vibrating tube densimeters have been used to measure the density of DIDP over the same pressure and temperature range. For atmospheric pressure measurements, a low pressure densimeter was used because it is more accurate, while a high pressure densimeter was used for high pressure measurements. More details on the instruments used are given in Chapter 3.

1.3 Fundamentals of viscosity:

As a prelude to further discussion on viscosity measurements, successive subsections are devoted to explaining its definition, importance, the effect of pressure and temperature on viscosity and finally the intrinsic nature of a fluid whose viscosity is to be measured.

1.3.1 Definition of Viscosity

Viscosity of a fluid can be pictured by assuming a confined fluid between two rigid plates where the top one is movable and the bottom one is stationary. When a shearing force F, a force that is applied tangentially on the boundary, is exerted on the top plate, causing it to move in the x-direction with a constant velocity v_0, the intermediate layers will flow at different velocities relative to each other. Hence, a velocity gradient $\frac{dv_x}{dz}$, sometimes known as shear

rate σ, will start to develop. The nearest layer of fluid to the top boundary will flow with a maximum value υ_0 the same as the top plate whereas the velocities of the in-between layers decrease in the z-direction towards the bottom plate, as shown in Figure 1.1.

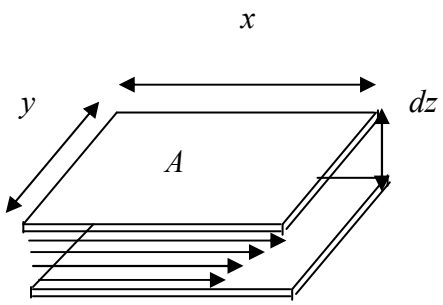

Figure 1.1: Simple sketch defining the coefficient of viscosity based on simple laminar flow.

If the flow is laminar (i.e. the fluid moves smoothly in layers), every shearing stress τ, the shearing force F divided by the layer area A over which it acts, opposing the relative motion of these layers, hence the negative sign, is proportional to the velocity gradient and is expressed by Newton's law as[6]:

$$\tau_{x,z} = \frac{F_{xz}}{A} = -\eta \frac{d\upsilon_x}{dz} = -\eta\sigma \qquad (1.1)$$

The proportionality coefficient η is known as the dynamic or absolute viscosity of the fluid or simply viscosity. Thus, viscosity is considered the main reason for the resistance of fluid motion. There are several factors that can greatly affect the viscosity such as temperature, pressure, composition and the type of fluid (Newtonian or non-Newtonian). As this thesis is concerned with pure Newtonian fluid, temperature and pressure dependency of this type of fluid only is considered and will be discussed in detail later.

1.3.2 Importance of Viscosity

The viscosity of a fluid is one of its main thermophysical properties and is of great significance for many scientific and industrial areas. It is a key factor that has to be considered when fluids are transported or pumped. For example, it is desirable to pump fluid in the petroleum industry through a pipeline into many processing units[7]. The flow rate of a pump and hence its performance relies significantly on the viscosity of the fluid being transferred, so it is essential for the viscosity to be known precisely. The power consumption of the pump is also controlled by the viscosity since the more viscous the fluid is, the more power the pump needs[7]. It determines the flow rate of many other applications such as extrusion, printing and spraying[8].

1.3.3 Different flows and types of fluid

As a rule of thumb, in order for any viscometer to be correctly used and therefore accurately acquire viscosity data, any theoretical requirements that have been assumed during the development of working equations for the viscometer should be fully satisfied[9]. For instance, the mathematical model for a capillary viscometer is not applicable if the fluid does not flow through it in a streamline pattern[9]. However, there are commonly two requirements for most viscometers that are considered most important. Theses will be discussed in depth in this subsection. The first is the type of flow of the fluid whose viscosity is being measured. This can be divided into two distinguishable classes: streamline or laminar and turbulent flow. Generally, either type is deemed as an irreversible deformation because the work done by the force causing the fluid to commence flow is not mechanically recoverable[8]. Figure 1.2 shows the most common laminar flows that can be found in viscometery. Case 1 represents flow behaviour that exists in a rotational viscometer, Case 2 exhibits the type of flow found in a capillary viscometer, while Case 3 shows the flow pattern in an oscillating-body viscometer[8].

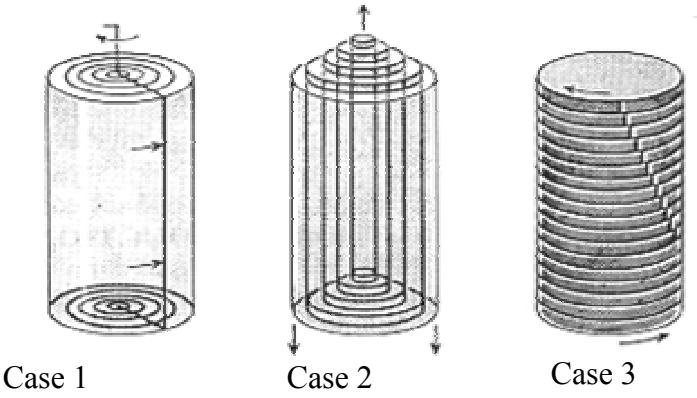

Figure 1.2: Diagrams showing various shapes of laminar flow

Reynolds[6] defined laminar flow of fluid when its particles move in a smoothly regular manner with no transfer of matter between layers. This behaviour of flow can only occur if the velocity of the flow does not exceed a maximum limit; whereas, beyond this point the flow evolves into a turbulent flow. In the case of turbulence, irregularities appear in the flow, and transfer of matter between layers occurs. However, on the basis of Reynolds' experiment, the flow pattern can be determined by a dimensionless quantity known as the Reynolds number Re, which is directly proportional to the mean velocity of the fluid and is given by[6]

$$\mathrm{Re} = \frac{\bar{\upsilon} d \rho}{\eta} \qquad (1.2)$$

Where $\bar{\upsilon}$ is the mean velocity of the fluid, d is a characteristic dimension of the system in which the fluid occurs and ρ and η are its density and viscosity respectively. Furthermore, it has been experimentally shown that most fluids will flow in a laminar way if the Reynolds number is less than 1000[10].

The second requirement is the type of fluid that characterises the behaviour of the fluid under stress. A fluid is said to be Newtonian when the shear stress τ is linearly dependent on the velocity gradient or share rate σ, i.e. obeying Newton's law. In other words, the viscosity is independent of the shear rate[6,7,11,12]. The majority of fluids are in this category. Newtonian fluid is depicted schematically in Figure 1.3.

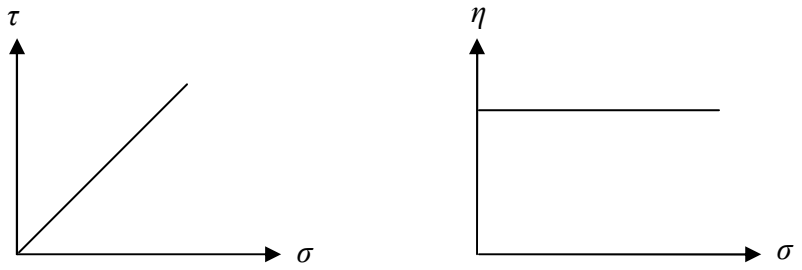

Figure 1.3: Simple sketches representing the relationship between the viscosity and shear rate and also between the shear stress and the shear rate.

The second type is Non-Newtonian fluids, which do not obey Newton's law and the viscosity of this type of fluid is dependent on the shear rate. Since this work is concerned with Newtonian fluid, no further discussion of Non-Newtonian fluids is presented.

1.3.4 Temperature and pressure dependence

The viscosity of a fluid is highly sensitive to parameters such as pressure and temperature[6,8,13]. The magnitude of this sensitivity depends on other factors associated with the fluid, for example, whether the fluid is a gas or a liquid. The discussion in this subsection is limited to the change of viscosity of liquids caused by the variation of temperature and pressure.

Several approaches and theories have been proposed over the years to describe and correlate the viscosity of a fluid as a function of temperature. Andrade's [11]theory is the most preferable among others because it is successful in correlating data over a cycle temperature range. According to this theory, liquid viscosities under isobaric condition are conceived to be due to the transfer of molecules' momentum between their layers in addition to cohesive forces between molecules. When the temperature is raised the cohesive forces tend to decrease and as a consequence the share

stresses decrease; simultaneously, a rise in temperature will lead to an increase in the rate of molecules being transferred so the shear stresses become raised. The final result of this process is that the viscosity of liquids declines with increasing temperature[6]. In 1930, Andrade exemplified the relation between the viscosities of a liquid and temperature by[11]

$$\eta_0(T) = \exp\left(e + \frac{f}{T}\right) \tag{1.3}$$

Where e and f are constants and can be obtained from fit to the data. T denotes an absolute temperature.

However, it should be pointed out that a third constant C was introduced by Vogel, then known as the Vogel equation, so Equation 1.3 becomes[13,14]

$$\eta_0(T, p)/\mathrm{mPa}\cdot\mathrm{s} = \exp\left\{e + \frac{f}{(T/\mathrm{K}) + g}\right\} \tag{1.4}$$

Equation 1.4 is widely known as the Vogel-Fulcher-Tammann equation or simply (VTF)[15]. It is widely recognised by most researchers; for example, it has been adopted by (NIST) as an accurate interpolation formula especially for the molten glass standards[11].

The second thermodynamic factor which affects the viscosity of a fluid is pressure[6,13]. The magnitude of the pressure effect is strongly dependent on the nature of the liquid and the viscosity of liquid, as a general trend, increase when the pressure increases[6]. For instance, the viscosities of most hydraulic oils used in hydraulic machinery increase by 10 to 15 per cent when the pressure is raised up to 70 bar[6]. On the other hand, water viscosity surprisingly almost doubles when the pressure is raised from 1 bar up to 1000 bar[6]. Another modified form of the Vogel-Fulcher-Tammann function has been used in this work to represent the viscosity of DIDP as a function of pressure and temperature. This equation is discussed in the next section.

1.4 Density and viscosity mathematical correlations:

For the purpose of comparison with literature data for viscosity and density values, several mathematical correlations were employed. For density measurements the modified Tait equation [16]was used, which is given by

$$\rho(T,p)=\rho_r(T,p_0)\left\{1-C\ln\left(\frac{B(T)+(p/\mathrm{MPa})}{B(T)+(p_0/\mathrm{MPa})}\right)\right\}^{-1} \qquad (1.5)$$

Where p_0 = 0.1 MPa, C is a constant, T is absolute temperature, ρ_r and $B(T)$ are exemplified by

$$\rho_r / \mathrm{kg \cdot m^{-3}} = \sum_{i=0}^{2} A_i \, (T / \mathrm{K})^i \qquad (1.6)$$

$$B(T) = \sum_{i=0}^{2} b_i \, (T / \mathrm{K})^i \qquad (1.7)$$

The coefficient Ai was obtained by fitting density data at atmospheric pressure to Equation 1.6 while bi and C were extracted from fitting density data at higher pressure to equation 1.5. These coefficients are given in Chapter 6.

For viscosity data, the following Vogel-Fulcher-Tammann VTF equations were used:

$$\eta_0 (T, p) / \mathrm{mPa \cdot s} = \exp\left\{ A + \frac{B}{(T / \mathrm{K}) + C} \right\}$$

This equation, previously mentioned, Equation 1.4, was used to correlate the viscosity measurements at ambient pressure as a function of temperature; whereas, the experimental data at various temperatures and pressures were fitted to the modified Vogel-Fulcher-Tammann function which, is empirically given by

$$\eta(T, p) / \mathrm{mPa \cdot s} = \exp\left\{ a + b(p/\mathrm{MPa}) + \frac{c + d(p/\mathrm{MPa}) + e(p/\mathrm{MPa})^2}{(T/\mathrm{K}) - T_0} \right\}, \qquad (1.8)$$

Where the coefficients A, B, C, a, b, c, e and T_0 were obtained from regression analysis and are given in Chapter 6.

Chapter 2

REVIEW OF VISCOSITY MEASUREMENT TECHNIQUES

2.1 Introduction:

A precise measurement of viscosity, as previously discussed, is crucially required in many fields, so numerous methods for obtaining it have been developed over the years. Generally, those methods involve a compromise between accuracy, simplicity of use and suitability for certain types of fluid or flow[8,9,11]. For the sake of brevity and simplicity, this chapter outlines and discusses various types of viscometers without resorting to mathematical complication. Further discussion about their types, advantages, disadvantages, operation modes and accuracy are also considered. For summary purposes, this chapter ends with a summary table.

In terms of accuracy, viscometers may be classified as primary or secondary[17], where the former is deemed more accurate than the latter. Furthermore, primary viscometers are designed on the basis that their working equations are complete or at least, if not, correction terms that are needed to compensate for the incompleteness are well-determined[17]. However, the underlying equations and/or the corrections for secondary viscometers are

incomplete or insufficiently known. Alternatively, viscometers can be generally divided into six types based on their geometrical designs and experimental techniques used[9,10]. These include capillary, rotational, oscillatory-body, falling-body and vibrating wire viscometers.

2.2 Capillary viscometer:

Capillary viscometers were one of the earliest widely used methods in viscometry. They are capable of obtaining the viscosity by two different approaches: absolute and relative[9]. The absolute mode is employed if the physical constants of the mathematical equation of the viscometer can be calculated sufficiently without recourse to calibration procedures. The relative approach is applied, in contrast, when these constants can only be accurately determined by using fluids of known viscosity, i.e. calibrating fluids[8,9]. However, viscosity can be measured when volumetric flow rate Q of a known volume of a fluid is measured by forcing this amount to travel a specific distance through the capillary tube by a known pressure drop. Its governing equation is[9]:

$$\eta = \frac{\pi a^4 \Delta P}{8 Q(L + na)} + \frac{m\rho Q}{8\pi(L + na)} \qquad (2.1)$$

Where a is the radius of the tube, $\triangle P$ is pressure drop along the tube, ρ is the fluid density, n and m are correction factors and L is the length of the tube.

The above equation was verified by Poiseuille in 1846 under the following assumption[9,12]:

(1) the capillary is straight and has a regular cross section.

(2) the fluid is not compressible so its density is deemed constant.

(3) the fluid is Newtonian.

(4) the temperature of the fluid is stable.

(4) the flow type of the fluid must be laminar.

(5) there is no slippage at the tube wall.

In a real measurement, it may be impossible to verify some of the above assumptions precisely so necessary corrections must be applied. Interestingly, it should be pointed out that the viscosity value of water, the sole primary standard, was internationally adopted after being determined by Swindells et al.[18] with an absolute capillary viscometer with an uncertainty of 0.25 %.

This class of viscometer can also be utilised in relatively extreme conditions such as high pressure and high temperature on the proviso that special additional instruments to those used in normal conditions and necessary precautionary measures are considered[9]. Furthermore, its availability, cheapness, simplicity of use and structure are other advantages[8,10,11]. However, it has some disadvantages; for instance, it demands a large amount of fluid, it is time consuming, it requires a number of calibrating fluids to cover a desired viscosity range[8], the measurements cannot be continuously made[10], and it is difficult to automate[4]. Its applicability being limited to Newtonian liquids is another drawback because serious error can be produced when it is used for non-Newtonian liquids[11]. It is sometimes desirable for online viscosity data to be taken, for example during pipeline operation, which the capillary viscometer obviously cannot support[7].

2.3 Rotational viscometer:

The operational principle of the rotational viscometer is based on the fact that when a rotor (e.g. cylinder, disk or cone) is immersed in a fluid and is rotated at a constant speed, the surrounding fluid causes a torque on its surface[8,9,11]. If such running torque can

produce a steady rotational motion, the fluid viscosity can be assumed to be directly proportional to the torque. The working equation that relates the torque to the viscosity depends mainly on the geometry of the viscometer[10]. There are numerous types of rotational viscometers[8]. However, they are most suitable for studying non-Newtonian fluids, since the shearing stress can be made constant throughout the fluid sample[10]. This consistency in shearing stress is the chief advantage over capillary viscometers. Rotational viscometers need a small sample and do not require bulk motion[9-11].

2.4 Oscillating-body viscometer:

The main idea of the oscillating-body viscometer is that when a suspended axially symmetrical body is immersed in a fluid medium, and then set to free harmonic oscillation motion, the body will exhibit a torque on its surface because the fluid resists its motion[8-10]. As a sequence of this resistance, a series of oscillations of decreasing amplitude will be observed, where the amplitude of each complete oscillation will be less and a constant fraction of the preceding one[10]. Therefore the logarithm of the period will differ from each other by a constant value, known as

logarithmic increase[10]. This effect can be used as a measure of the viscosity. In other words, the viscosity can be related to both the oscillating period and the logarithmic decrement and can be extracted with the aid of reliable working equations[9]. These equations have been derived for certain shaped bodies and under certain assumptions, so they are valid on the condition that those assumptions are sufficiently realised[8,9]. Cylinders, spheres and disks are some examples of these bodies and the ones most commonly used. This type of viscometer has been successfully used in both gases and liquids[9], over various conditions of temperature and pressure. Although this type of viscometer is very easy to mechanically construct and is capable of coincidentally measuring the fluid density and viscosity, its accuracy is hindered by the difficulties of developing an exact mathematical treatment[11]. However, an approximate mathematical treatment can be obtained but some correction terms must be considered, for example, outer boundary correction, second flow and variations of fluid compressibility owing to pressure changes[8]. The interested reader is referred to references[8,9].

2.5 Falling-body viscometer:

A falling-body viscometer can be used to measure fluid viscosity by determining the elapsed time of free-fall of a shaped body travelling a specific distance, where this time is directly related to the fluid viscosity[12]. In other words, the more viscous the fluid the more time the body takes to travel the distance. Commonly, spheres and cylinders are the two most well-known shapes of bodies. A simple schematic illustration is shown in Figure 2.1.

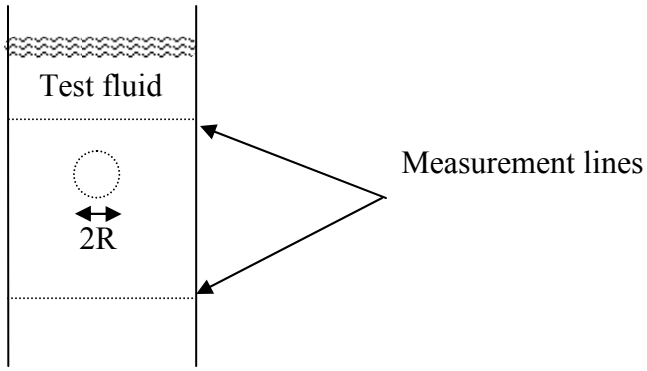

Figure 2.1: Simple sketch illustrating a falling sphere viscometer.

According to Stokes' law, if a sphere falls slowly through an incompressible Newtonian fluid of infinite extent and at constant velocity *v*, the viscosity η of the fluid can be extracted from the following equation[9,10]

$$\eta = \left(2/9\right)(\rho_s - \rho)gR^2 v = \left(2/9\right)\frac{(\rho_s - \rho)gR^2 t}{L} \qquad (2.2)$$

Where g is the fall free constant, R is the radius of the body, t is the time of fall through distance L and ρ_s is the density of the sphere and ρ is the density of the fluid. An additional requirement is that the Reynolds number, Re=$2R\nu\rho/\eta$, is much less than one[9]. There are two practical obstacles that hinder the applicability of the above equation and consequently the employment of this type of viscometer[11]. These obstacles result from the assumptions the theory not being able be fully satisfied. The first one is that it is practically impossible to have fluid of infinite extent, i.e. the fluid is unbounded. It is usually known as the wall effect. The second obstacle is that it is hard to attain the Reynolds number smaller than unity unless small spheres are used in a high viscous medium, which means that the viscosity measurements will be limited to a small range. Although the second obstacle has been satisfactorily solved by considering a cylindrical configuration, the correction factor associated with the working equations is the main disadvantage[10]. Other shortcomings are that the falling-body viscometer cannot continuously measure the viscosity of a fluid, for example, when the viscosity changes due to a variation of

temperature or pressures; so different size of spheres have to be employed[8]. It is generally not recommended for non-Newtonian fluids[8]. However, it is generally most suitable for high pressure measurement and for reasonably viscous material[9].

2.6 Vibrating wire viscometer:

Vibrating wire viscometers are different from the oscillating-body viscometers in the way that their oscillating motion is transitional whereas the oscillating-body motion is rotational[19]. When a taut wire, immersed in a fluid medium, is driven electromagnetically over its first resonance frequency, its resonance curve width can be related to the fluid viscosity[4,20]. If a buoyant mass is attached to one end of the wire, the density of the fluid can be calculated with the aid of theoretical working equations[4,21,22]. Thus such a device can be employed to measure the viscosity and the density simultaneously. The significantly essential feature of this device is that its working equations are complete under some attainable assumptions, in view that these equations have been rigorously developed[20]. Thus, such a device, unlike other types of viscometers, requires no boundary corrections. It also requires no bulk motion of a body or the fluid and can be used for different

fluid phases such as mixtures and gases[4]. Furthermore, it is of simple mechanical construction and can be automated and operated over extreme conditions of temperatures and pressures[4]. However, the vibrating wire viscometer is not available commercially, since it is very specialized instrument and hence it is used in a few research institutes around the word[17].

The main points of its theory and its working equations are fully developed in Chapter 4, so only its advantages and operating modes are discussed here. An electromagnetic coupling is used to set the wire into transitional oscillating motion and coincidentally to record the induced voltage due to its motion. Such coupling can be made by placing a wire perpendicularly in a uniform magnet field and then feeding an alternative current to the wire. Thus, an electromotive force, due to an interaction between the current and the magnetic field, drives the wire transversely around its rest position. If the current is continually provided to the wire at constant amplitude but at different frequencies, the viscometer is operated in the frequency domain[4]. Alternatively, another operation mode, transient mode, can be utilized when the current is passed for only a short time and then switched off. Therefore, the decay time of the oscillations owing to the viscosity of the fluid is a

measure of the viscosity, where the more viscous the fluid is the less the decay time is[4,23].

2.7 Summary:

In the review of the foregoing information, it can be judged that the criteria upon which the viscosity device, among those discussed previously, should be chosen depend on several factors. These factors are given in Table 2.1. Although the accuracy of the device has not been considered among the above criteria, owing to its dependency on other factors, the vibrating wire and the oscillating viscometers are deemed, along with calibrated capillary viscometer, to more accurate[17].

Table 2.1: A comparison table between the main viscometers types.

Criterion	CP[1]	FB[2]	OB[3]	VW[4]	RV[5]
Cost	low	low	high	high	low
Working equation	simple	simple	complicated	simple	simple
Sample size	large	large	small	small	small
working condition	quite high	extreme	extreme	extreme	low
Free of corrections factor	no	no	yes	yes	no
Continuous measurement	no	no	yes	yes	no
Bulk motion of fluid	required	not required	not required	not required	not required
previous knowledge of fluid density	not required	required	required	required	not required
Fluid phase used	gas and liquid	liquid	gas and liquid	gas and liquid	liquid
Time consumption	much	much	less	less	less

Table 2.1 continued

Criterion	CP[1]	FB[2]	OB[3]	VW[4]	RV[5]
Type of fluid	N[6] and non[7]	N	N	N	N and non
Commercial status	available	available	not available	not available	available

1 CP denotes Capillary viscometer.
2 FB denotes Falling-body viscometer
3 OB denotes Oscillating-body viscometer
4 VW denotes Vibrating wire viscometer
5 RV denotes Rotational viscometer
6 N denotes Newtonian fluid
7 non denotes non-Newtonian fluid

Chapter 3

LITERATURE REVIEW

As a preliminary response from The Bureau International des Poids et Measures (BIPM) in cooperation with the International Association of Transport Properties to the continued industrial demand for identifying viscosity reference fluids in the range of (100 to 200 mPa·s), several research groups have instigated a study of the adequacy of a range of proposed fluids as well as establish reference values of their viscosities. In 2004, under the aegis BIPM, Caetano et al.[3] reported the first viscosity measurements on Diisodecylphthalate (DIDP) as one proposed candidate fluid as a suitable reference. These measurements were performed on one sample of DIDP, 99.5 % nominal purity, at atmospheric pressure and in a narrow range of temperature, from 288.32 K to 308.12 K with an estimated uncertainty of less than ±1.5%. According to them, the major contribution to this uncertainty was mainly due to the calibrating fluid, toluene at near 298 K and at 0.1 MPa, which had been used to determine an effective value of the wire radius of their viscometer. In 2005, another measurement was made by the same researchers [24], using a different calibrating fluid as a step to

improve the viscometer performance and hence reduce the uncertainty. They used water, the ultimate viscosity reference fluid, to establish direct traceability and consequently acquired an overall uncertainty of the order ±1 %. These later experimental measurements were taken over a slightly increased range of temperatures by approximately 10 K. Furthermore, density measurements over the same range were also included because had been lacking and are required to derive the kinematic viscosity. The expanded uncertainty of the density data was stated to be ± 0.1 %. In a third paper by Caetano and coworkers [25], the water content and the purity of the sample were investigated since these data are necessary for the acceptance of DIDP as a moderate viscous standard. In this paper, the water content effect on the density and the viscosity of two DIDP samples of different impurity was reported. As a summary, it was stated that the water effect does not cause a dramatic change to the density values whereas when the content of water was raised by a factor of five its viscosity dropped by about ± 0.5 %, but this was probably within the uncertainty of the measurements.

Recently, Harris et al.[26] have published new viscosity data on DIDP at pressures up to 1 GPa and at temperatures between (0 and

100) ^{o}C. Three types of high pressure falling-body viscometers were exploited to study three different grades of DIDP which were obtained from various sources. The purities of the samples were 99 %, 99.5 % and 99.8 %. Density data were also reported at ambient pressure over the same temperatures of viscosity measurement. All the samples were dried over a $3A^{0}$ molecular sieve for several weeks. The uncertainty in the viscosity data was stated to be 1 % whereas the uncertainty of the density measurements was assumed to be ± 0.05 kg/m^{3}.

For the sake of brevity, all the preceding information of the measurements of the viscosity of DIDP is summarized in Table 3.1.

Table 3.1: Review of the literature on the measurement of density and viscosity of DIDP along with the temperature and pressure range, cited uncertainty, sample source, water content, method used* and the nominal purity.

Year	$\frac{T_{min} - T_{max}}{K}$	$\frac{P_{max}}{MPa}$	$\frac{Purity}{\%}$	Method*	Uncertainty	Property	Source	$\frac{Water\ content\ w}{10^{-6}}$	Calibrating fluid	Treatment**	Ref
2004	288 - 308	0.1	99.5	VW	±1.5 %	viscosity	Merck P.a	20	toluene	yes	[3]
2005	283 - 313	0.1	99.5	VW	± 1.0 %	viscosity	Merck	20	water	yes	[24]
2005	283 - 313	0.1	99.5	VTD	± 0.1 %	density	Merck	20	not stated	yes	[24]
2006	293 - 298	0.1	99.8	VW	± 0.8 %	viscosity	Merck	107	water	no	[25]
2006	293 - 298	0.1	99.8	VTD	± 0.1 %	density	Merck	107	not stated	no	[25]
2006	273 - 353	0.1	99.0	FB	± 1.0 %	viscosity	Merck	unspecified	not stated	yes	[26]
2006	273 - 348	800	99.8	FB	± 1.0 %	viscosity	Merck	unspecified	not stated	yes	[26]
2006	273 - 338	1000	not stated	FB	± 1.0 %	viscosity	ABCR GmbH	unspecified	not stated	yes	[26]

Table 3.1 continued

Year	$\frac{T_{min} - T_{max}}{K}$	$\frac{P_{max}}{MPa}$	$\frac{Purity}{\%}$	Method*	Uncertainty	Property	Source	$\frac{Water\ content}{ppm}$	Calibrating fluid	Treatment**	Ref
2006	273 - 363	0.1	99.0	VTD	± 0.05 Kg/m^3	density	Merck	unspecified	not stated	yes	[26]
2006	273 - 363	0.1	99.8	VTD	± 0.05 Kg/m^3	density	Merck	unspecified	not stated	yes	[26]

* For viscosity data either vibrating wire (VW) or falling-body (FB) viscometer was used and for density data vibrating tube densimeter was used (VTD)

** Using a molecular sieve for drying.

Chapter 4

THEORY AND CALCULATION PROCEDURE

4.1 Theory:

A theoretical study of the oscillating motion of a straight stretched wire when it is surrounded by a fluid was the starting point of the development of vibrating wire viscometery. In 1963, Tough et al.[27] used this study to develop the first vibrating wire viscometer to measure the viscosity of helium liquid. Since then, this class of viscometer has evolved remarkably in various directions such as in its measurement range, validation over extreme conditions of temperature, pressure, as well as design and operating approaches. Since the hydrodynamic theory of the surrounded fluid and the mechanical theory of the wire have been extensively studied and reported in detail by several researchers[4,17,20,21], only the main points and the most important equations are reported below.

According to Retsina et al.[20], when a thin circular-section wire of length 2L clamped at both ends is immersed in a Newtonian fluid and set to vibrate transversely around its rest position, as shown schematically in Figure 4.1, provided appropriate assumptions are

satisfied, its velocity at any time can be obtained from

$$v = \frac{\partial y}{\partial t} = \frac{fFi}{m_s \pi \left[f_0{}^2 - (1+\beta) f^2 + (\beta' + 2\Delta_0) f^2 i \right]} \qquad (4.1)$$

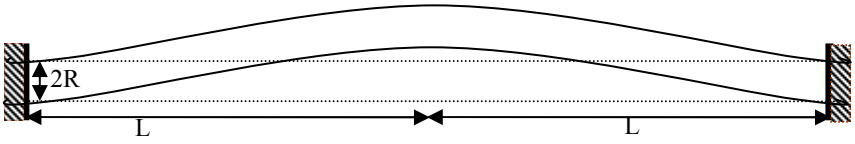

Figure 4.1: Simple drawing represents the vibrating wire.

Where y is the transverse displacement, F is the amplitude of the magnitude of the driver force per unit length, m_s is the wire mass per unit length, f is the frequency and $\triangle_0$ is the internal damping factor that accounts for the wire material inelasticity and magnetic damping. β' and β account for added mass and damping owing to the presence and the acceleration of the fluid. They are defined by the following equations[4,5,20]:

$$\beta = k \frac{\rho}{\rho_s} \qquad (4.2)$$

$$\beta' = k' \frac{\rho}{\rho_s} \qquad (4.3)$$

Where ρ and ρ_s are the fluid and the wire density respectively, k and k' characterise the fluid flow around the wire and are functions of a complex parameter $\boldsymbol{A}$. They are expressed mathematically as

$$k = -1 + 2\,\mathrm{Im}(\boldsymbol{A}) \tag{4.4}$$

$$k' = 2\,\mathrm{Re}(\boldsymbol{A}) \tag{4.5}$$

$$\boldsymbol{A} = i\left[1 + \frac{2\,\mathrm{K}_1(\sqrt{i\Omega})}{\sqrt{i\Omega}\,\mathrm{K}_0(\sqrt{i\Omega})}\right] \tag{4.6}$$

The parameters K_1 and K_0 are modified Bessel functions and the quantity Ω is closely connected to the Reynolds number and is a function of the resonance frequency *f*, the radius of the wire *R*, the density and the viscosity of the fluid, which is expressed as

$$\Omega = \frac{2\pi f \rho R^2}{\eta} \tag{4.7}$$

Assumptions were imposed when the above equations were derived, owing to mechanical and hydrodynamical theory treatments, so as a consequence the following requirements relating to the behaviour of the sensor, physical requirements, and to the geometry and experimental requirements of the device must be fulfilled:

1. According to the mechanical theory, the wire was assumed to be infinitively long, stretched, stiff, and free of shearing deformation. This assumption is satisfied provided that the wire length is much

greater than its radius (i.e. the ratio between the wire radius and its length must be of the order of 0.001)[5].

2. The maximum dimensionless amplitude of the oscillation ε that characterises the linear behaviour of the wire must be less than the wire radius R. In other words[4,17,28,29],

$$\varepsilon = \frac{y_{\max}}{R} << 1 \qquad (4.8)$$

Where $y_{\max}$ is maximum displacement of the wire.

3. The postulate of neglecting the compressibility effect of the fluid, which was introduced by the hydrodynamical theory, is allowed when Mach number Ma is small i.e.[17,19,28],

$$\mathrm{Ma} = \frac{2\pi f\varepsilon}{c} << 1 \qquad (4.9)$$

Where the c is the sonic velocity in the fluid.

4. In the mathematical treatment the fluid was considered to be unbounded, but in practice the fluid is contained in a vessel. Thus, an additional effect, the boundary effect, must be added which results in an increase in the uncertainty of the viscosity value. This uncertainty can be reduced to the order of 0.5 % on the condition that the inner radius of the vessel R_v is large in comparison with

the wire radius R. Typically, $\frac{R_V}{R} << 45$ for Reynolds number <100[4,5]. The Reynolds number is the quantity that determines whether the flow is viscous or turbulent. The aforementioned theoretical requirements have been well realised for the viscometer used in this work.

4.2 Viscosity calculation procedure:

In practice, to make use of equations, (4.1) to (4.7), for calculating the viscosity of the fluid, an appropriate method has to be employed to cause a taut metallic wire of electrical impedance r to vibrate at a frequency f and then measure the wire's transverse velocity v. This can be achieved by placing the wire perpendicularly to a permanent uniform magnetic field of strength B and then passes an alternative current I of a suitable frequency f. An electromagnetic interaction between the current and the magnetic field will create a magnetic force that consequently will drive the wire into transverse motion with velocity v. simultaneously, an induced electromotive force $\boldsymbol{V}_I$, the Lorentz force, is generated along the wire as a result of this transitional motion. This induced voltage is directly proportional to the wire

velocity and therefore, it is a measure of it. The amplitude of the magnetic force per unit length is given by[4,23]

$$F \approx IB \qquad (4.10)$$

While the induced voltage can be calculated from Faraday's law of induction as follows:

$$\boldsymbol{V}_1 = B\,v\,L \qquad (4.11)$$

Substituting equations 4.10 and 4.1 into 4.11 gives $\boldsymbol{V}_1$ as:

$$\boldsymbol{V}_1 = \frac{\Lambda f i}{{f_0}^2 - (1+\beta) f^2 + (\beta' + 2\Delta_0) f^2 i} \qquad (4.12)$$

Where $\Lambda = 2ILB^2/\pi^3 \rho_s R$ is related to the amplitude of the oscillation[4,5].

The developed voltage across the wire is a complex voltage $\boldsymbol{V}$ which consists of two components. They are namely, the induced voltage $\boldsymbol{V}_1$ arising from the wire motion in the presence of the magnetic field, and $\boldsymbol{V}_2$ simply resulting from the impedance of the wire material. They can be mathematically represented by

$$\boldsymbol{V} = \boldsymbol{V}_1 + \boldsymbol{V}_2 \qquad (4.13)$$

$\boldsymbol{V}_2$ is given by[30]:

$$\boldsymbol{V}_2 = a + bf + ic + idf \qquad (4.14)$$

The adjustable parameters *a, b, c*, and *d* are related to the electrical impedance of the wire and the offset used in the lock-in amplifier. This is discussed in more detail chapter 6.

The complete mathematical model for the complex voltage $\boldsymbol{V}$, which is measured by the lock-in amplifier, is obtained by combining equations 4.12 and 4.14 as

$$\boldsymbol{V} = a + bf + ic + idf + \frac{\Lambda f i}{{f_0}^2 - (1+\beta) f^2 + (\beta' + 2\Delta_0) f^2 i} \qquad (4.15)$$

The viscosity is obtained by regression using the Levenberg-Marquardt technique, of the experimentally measured values of the complex $\boldsymbol{V}$ over a range of frequencies at which the wire is driven. In other words, the parameters Λ, f_0, *a*, *b*, *c*, *d* and the viscosity η are adjusted until the experimentally determined values of the complex voltage become sufficiently consistent with the voltage values obtained from Equation 4.15.

Since the aforementioned working equations require previous knowledge of the internal damping factor $\triangle_0$, the wire density ρ_s and radius of the wire *R*, a calibrating fluid, toluene, was employed for the determination of *R* whereas $\triangle_0$ was determined from the measurement of the resonance curve in vacuum. ρ_s was taken from the literature. These values are summarized in Table 4.1:

Table 4.1: Key parameters used in the working equations

Parameters	Value	Source
$\triangle_0$	$122 \cdot 10^{-6}$	determined from vacuum measurement
ρ_s/Kg.m^{-3}	19300	literature
R/mm	0.0723	determined used toluene
L/mm	40	measured

Prior to performing the regression, the real part of experimental data of the complex voltage V was fitted to a 'normalized' Lorentzian type equation. This was done to predict the maximum dimensionless amplitude of the oscillation ε, the fundamental resonant frequency f_r and one half the width of the resonance peak at a frequency $1/\sqrt{2}$ times that of the maximum amplitude g, where g was used for determining the frequency range over the resonant frequency of the wire, as explained in details in Chapter 6.

Chapter 5

EXPERMENTAL

5.1 The vibrating wire apparatus:

The vibrating wire viscometer used in this work had been previously designed and constructed in the Chemical and Process Engineering Department at the University of Canterbury. It consists of a tungsten wire as an oscillating probe, a holder tube, two magnet blocks in the shape of a rectangle, a magnet assembly, a high pressure sealing gland and a pressure vessel. A schematic cross section of the apparatus is shown in Figure 5.1 and Figure 5.2.[4]

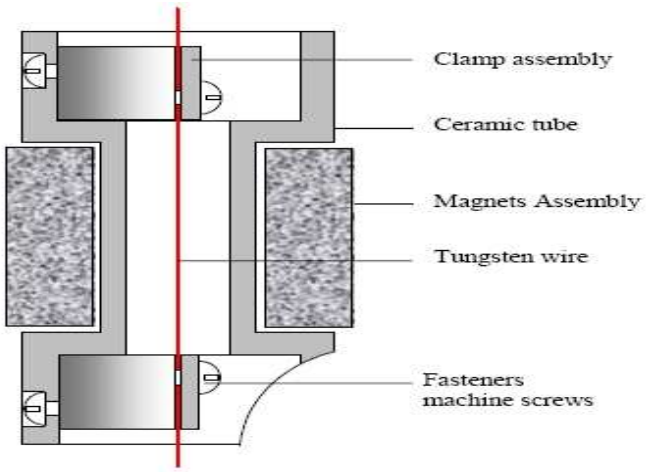

Figure 5.1: A diagrammatic cross section of the main parts of the vibrating wire viscometer.

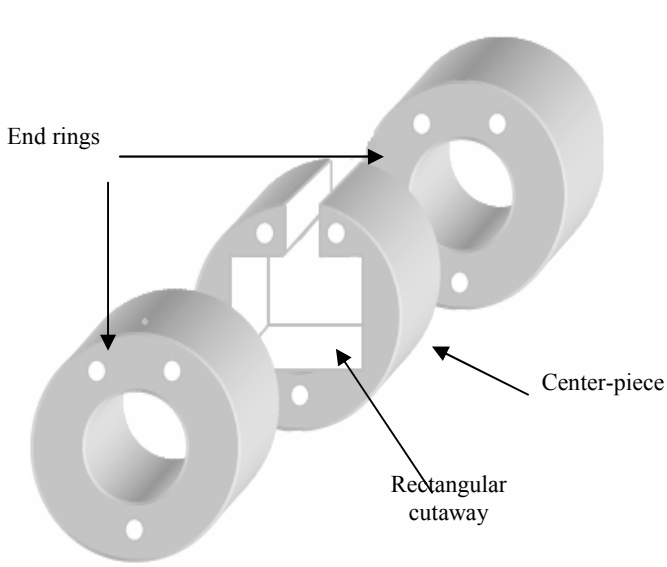

Figure 5.2: Sketch of the magnetic configuration for holding the magnets, composed of three non-magnetic stainless steel pieces, namely two end rings and one center-piece with a rectangular cutaway.

The wire, made of tungsten, was nominally 40 mm long and 0.15 mm diameter. Tungsten was preferred and chosen because of its good features, namely, a high Young's modulus $E \approx 411$ GPa and high density $\rho_s = 19300$ Kg·m^{-3}. The first feature maintains high stability for the resonance while the second feature makes the wire more sensitive to the surrounding fluid. It was supplied by Goodfellow™, UK, with purity greater than 99.95 %. The wire was inserted inside the non-magnetic holder tube, the machinable ceramic tube, and then the top end was tightened to the tube with

the aid of a non-magnetic clamp. After that the wire was tensioned from the bottom end by attaching a mass to it for approximately 24 hours before the mass was removed. The bottom end was then tightened gently to the tube. This mass was inferred from Equation 5.1, which allowed us to determine the preferred fundamental resonance frequency f_r to be obtained[4,5]:

$$f_r = \frac{1}{2L}\sqrt{\frac{mg}{\rho_s \pi R^2}} \qquad (5.1)$$

where L is the wire length, g is acceleration of the free fall, m is the mass and R is the radius of the wire. Ceramic material was selected for the tube because it was deemed to be a perfect insulator, its electrical resistively $\approx 10^{16}$ Ω·m, hence the two ends of the wire were electrically isolated from each other. The magnet holder was constructed from three pieces, as shown in Figure 5.2, where the middle piece has a rectangular cut-away so that the magnet blocks could be easily accommodated while the other pieces, in the form of rings, were used to clamp both the tube and the middle piece. The magnets, Sm_2 (Co, Fe, Cu, Zr, Hf) $_{17}$, were obtained from Magnet Sales & Services™, UK, with a nominal length of 31 mm. They provided a magnetic field to the wire of approximately 0.3 T. The ratio of the wire length to that of the magnet was calculated to

sufficiently suppress the second and the third harmonic oscillations. This type of magnet, Sm_2 (Co, Fe, Cu, Zr, Hf) $_{17}$, was preferable because its operating temperature is 623 K and its reversible temperature coefficient of induction, ≈ -0.0004 K^{-1}, is very low. The former feature enhances the operating temperature range of the viscometer while the latter feature maintains an almost constant field strength regardless of any increase in temperature. After the two magnet blocks had been inserted into the rectangular cutaway which exists in the center-piece of the magnet configuration, shown in Figure 5.2. , the holder tube was placed in between them and then secured by the two end rings. The pressure vessel was designed to withstand pressure up to 60 MPa at 160 ^{0}C and the assembled vibrating wire viscometer was placed inside it. The vessel was made of non-magnetic austenitic stainless steel grade 316. The fluid under measurements flowed into and out of the vessel by the aid of two ports located at the top and bottom of the vessel.

5.2 The vibrating tube densimeter:

The density data were measured by utilising two Anto Paar DMA vibrating tube densimeters (Models 602 H and 512 P) for low pressure and high pressure measurements respectively. Prior to

commencing measurements, their calibrating constants were determined by employing a calibration procedure. For Model 512 P, the calibration was done with octane and water and then it was checked against toluene, the third fluid. The densities of toluene were obtained from ref 32 and those for water were taken from ref 1 and 31 while octane densities were calculated from the data reported in ref 17. For Model 602 H, vacuum and water were used for performing the calibration and then its parameters were validated with measurements on toluene. Although their operating principles are the same, in the low pressure densimeter the U-tube was made of glass and it is more accurate. When the U-tube is filled with fluid of density ρ and then excited to oscillate, the natural resonance frequency of the tube changes as the density of the fluid changes. Thus, the period of the oscillation, T, can be empirically related the fluid density by the following equation

$$\rho = A \cdot T^2 - B \qquad (5.2)$$

where constants A and B are found by calibration.

5.3 Temperature and pressure measurements:

Temperature was monitored by two industrial platinum resistance thermometers. One of 100 Ω nominal resistance was used for measuring the densimeter temperature while the other, with 50 Ω

nominal resistance, was utilised for measuring the temperature of the viscometer. The former was calibrated by comparison with a standard 25 Ω platinum thermometer which itself had been calibrated on the ITS-90 scale at the National Measurement and Calibration Laboratory in Saudi Arabia. The latter was also calibrated in the Chemical and Process Engineering Department at the University of Canterbury against a standard platinum thermometer calibrated at Measurement Standard Laboratory of New Zealand. For both density measurements, with low pressure and high pressure densimeters, the uncertainty of temperature was estimated to be ± 0.02 K, while for viscosity measurement it was estimated at ± 0.01 K. Pressures were produced by two hydraulic pumps and were measured with two dial gauges (Heise, Stratford,CT, models CM12524 and CM18357) as shown in Figure 5.3. They both had resolutions of 0.1 MPa and uncertainties specified as ± 0.25 MPa and ± 0.1 MPa respectively. The former was used for the viscosity measurements while the latter was used for density measurements.

5.4 Experimental setup:

As shown below in Figure 5.3, the vibrating wire was placed in the pressure vessel and they were both immersed in an oil thermostatic

bath, (Julabo, model FK3-ME). The bath was controlled with precision of ± 0.01 ^{0}C. One electrical lead was attached to each end of the wire that passed through a high pressure electrical feedthrough sealing gland, which was capable of holding the pressure inside the vessel, to a lock-in amplifier. The electrical feedthrough was obtained from Conax Buffalo™. Another oil circulating bath (Julabo, model FK3-ME) was connected to the high pressure densimeter for obtaining the desired temperature.

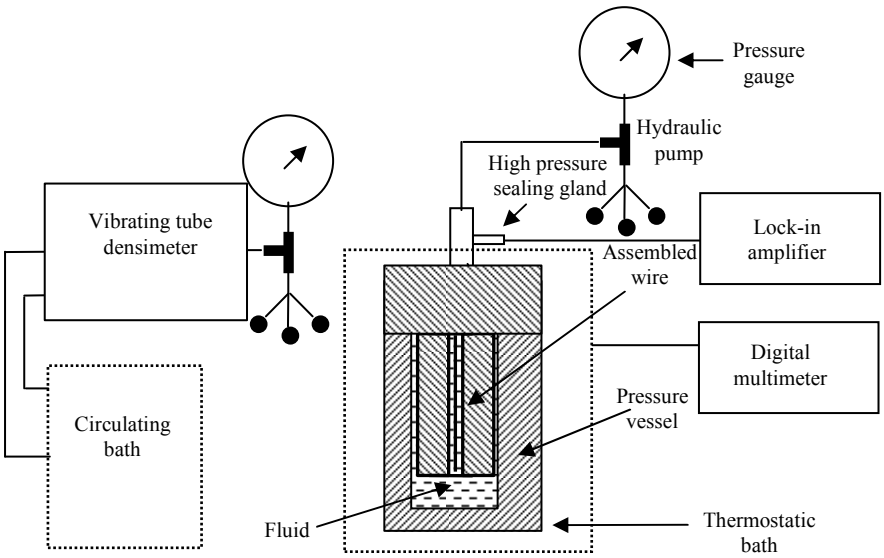

Figure 5.3: Schematic diagram showing the experimental setup for viscosity and density measurements

5.5 Fluid samples:

Three samples of DIDP were used. For simplicity we shall name them A, B and C. The suppliers provided chemical purities for each

sample but, in the absence of clear statements by the suppliers, it was assumed these are cited as mass fractions. Sample A was supplied by Fluka (lot no. 1228727) with a minimum stated purity of 0.998 that was the same purity but different source to that of Caetano *et al*.[24] Sample B was purchased from Merck KGaA with a nominal stated purity of 0.995 that is same purity but different source as that used by Caetano *et al.[3]* its lot no. was K22132622. Sample C was also obtained from Merck KGaA (lot number S4429432) with stated purity of 0.99.

5.6 Water content measurements:

The DIDP samples were dried over 0.4 nm activated molecular sieves for several weeks prior to use. The activation was done by rinsing the molecular sieve with water several times and then heated at a temperature of about 500 K under vacuum. DIDP is partially hydrophilic and consequently the mass fractions of water w in each of the samples as received were determined by Karl Fisher titration using a Radiometer Analytical Titrator, TIM 550 with the results: $w(\mathrm{A}) = 115 \cdot 10^{-6}$; $w(\mathrm{B}) = 417 \cdot 10^{-6}$; and, $w(\mathrm{C}) = 236 \cdot 10^{-6}$. The water mass fraction of water in each of these dried samples were also determined by Karl Fischer titration to be as follows: $w(\mathrm{A}) = 20 \cdot 10^{-6}$; $w(\mathrm{B}) = 24 \cdot 10^{-6}$; and $w(\mathrm{C}) = 29 \cdot 10^{-6}$.

5.7 Generating signal and data acquisition system:

The vibrating wire viscometer was operated in the forced mode in which a sinusoidal current of constant amplitude was passed through the wire over a frequency range. As shown in Figure 5.4, the lock-in amplifier (PerkinElmer™ model 7265), generated a sinusoidal signal which was then converted to an ac current of a constant amplitude by connecting a 1 KΩ resistor in series to the wire. The frequency of the driving signal was varied and stepped across the resonant region, (a detailed explanation is provided in subsection 5.7.1), with the aid of the lock-in amplifier's synthesizer (Sync). The complex voltage signal V, which includes the motional emf, was measured via connectors A and B, as shown in Figure 5.4., and recorded along with the frequency.

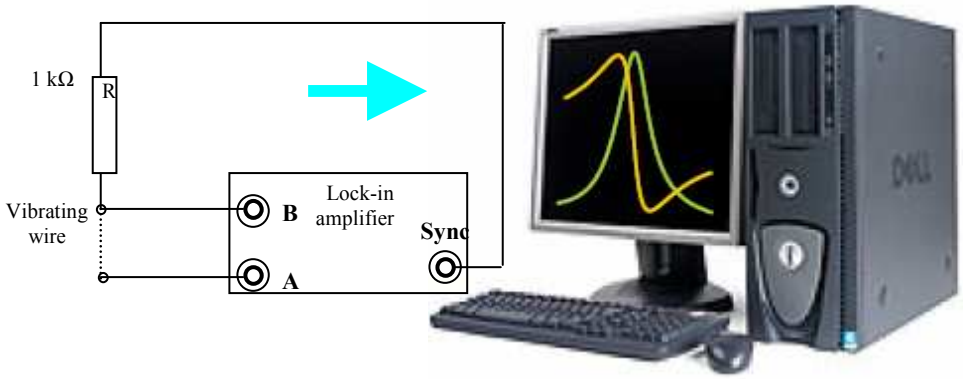

Figure 5.4: Schematic diagram illustrating the data acquisition system

The signal was transferred to the computer via a general purpose interface bus board (GPIB) which was controlled by special software. The MathCAD software was used for performing the calculation and the regression procedure.

5.7.1 Frequency range

The frequency range generated by the lock-in amplifier's synthesizer was swept twice, backward and forward, across the resonant region of the vibrating wire. This range was selected to be ($f_r \pm 5g$), where f_r is the fundamental resonance frequency and g is half the resonance line width at a frequency 0.707 ($\frac{1}{\sqrt{2}}$) times that of the maximum amplitude. The frequency scan started at (f_r-5g) with positive increments up to (f_r + 5g) and then backward with negative increments back to the starting point. The scanning time, backward and forward, was approximately 200 s. The half resonance width g was estimated by fitting the real part of the complex voltage $\boldsymbol{V}$ to a 'normalized' Lorentzian type equation.

However, prior to recording the complex voltage, the majority of the contribution coming from the drive voltage $\boldsymbol{V}_1$ was backed out by adjusting the lock-in amplifier offset voltage $f < (f_r - 5g)$.

Chapter 6

RESULTS AND DISCUSSION

6.1 Results for density:

The densities of sample B which were obtained from a vibrating tube densimeter (DMA 512 P) at temperatures T and at atmospheric pressure are listed in Table 6.1., while those at $p > 0.1$ MPa are given in Table 6.2. These measurements were made on sample B without treatment where the water mass fraction w was $417 \cdot 10^{-6}$.

Table 6.1: Experimental densities ρ_r obtained with a vibrating tube densimeter (DMA 512 P) of sample B with water mass fraction $w(\mathrm{B}) = 417 \cdot 10^{-6}$ at temperature T and p=0.1 MPa.

T/K	p/MPa	ρ_r/kg·m^{-3}
298.15	0.1	960.1
313.15	0.1	941.6
323.15	0.1	924.3
348.15	0.1	907.0

Density data ρ_r shown in Table 6.1 were fitted to the polynomial eq 1.6, with a standard deviation of the mean $100 \cdot \sigma(<\rho_r>)/\rho_r$ of ± 0.015 and the resulting parameters were: A_0 = 1228.371, A_1 = -1.05498 and $A_2 = 5.20 \cdot 10^{-4}$.

Table 6.2: Experimental densities ρ obtained with a vibrating tube densimeter (DMA 512P) of sample B with water mass fraction $w(B) = 417 \cdot 10^{-6}$ at temperature T and p >0.1 MPa.

298.15 K			
p/MPa	ρ/kg·m^{-3}	p/MPa	ρ/kg·m^{-3}
5	962.8	30	976.0
10	965.6	50	985.5
20	970.8	70	995.2
323.15 K			
5	945.4	30	960.4
10	948.5	50	970.7
20	954.6	70	980.1

Table 6.2 continued

373.15 K			
p/MPa	ρ/kg·m^{-3}	p/MPa	ρ/kg·m^{-3}
5	911.1	30	929.0
10	914.8	50	941.0
20	922.1	70	952.1
398.15 K			
5	893.4	30	913.5
10	898.8	50	926.0
20	906.6	70	938.9
432.15 K			
5	877.5	30	898.6
10	881.6	50	912.6
20	890.4	70	926.7

Table 6.2 continued

298.15 K			
p/MPa	ρ/kg·m^{-3}	p/MPa	ρ/kg·m^{-3}
5	962.8	30	976.0
10	965.6	50	985.5
20	970.8	70	995.2
323.15 K			
5	945.4	30	960.4
10	948.5	50	970.7
20	954.6	70	980.1
348.15 K			
5	927.9	30	944.1
10	931.3	50	955.3
20	938.0	70	965.7

Density values ρ at temperature T and p >0.1 MPa presented in Table 6.2 were fitted to the modified Tait equation, eq. 1.5, with a standard deviation of $100 \cdot \sigma(<\rho>)/\rho = \pm 0.1$ and the coefficients obtained by a least square fit were $b_0 = 295.7572$, $b_1 = -0.299083$, $b_2 = -0.000343$ and $C = 0.111608$.

This sample with this water content was used for the majority of the measurements as it is the most readily available commercial sample and there would be considerable practical advantages if it could be used without drying. The experimental densities listed in Table 6.2 are shown in Figure 6.1 as deviations from the values calculated from eq 1.5. The absolute maximum deviation was 0.24%. These differences are within the expanded uncertainty of the measurements which was estimated to be ±0.3 %. This uncertainty was evaluated on the basis of a comparison of the measured and literature values of the third fluid, as discussed in Chapter 6.

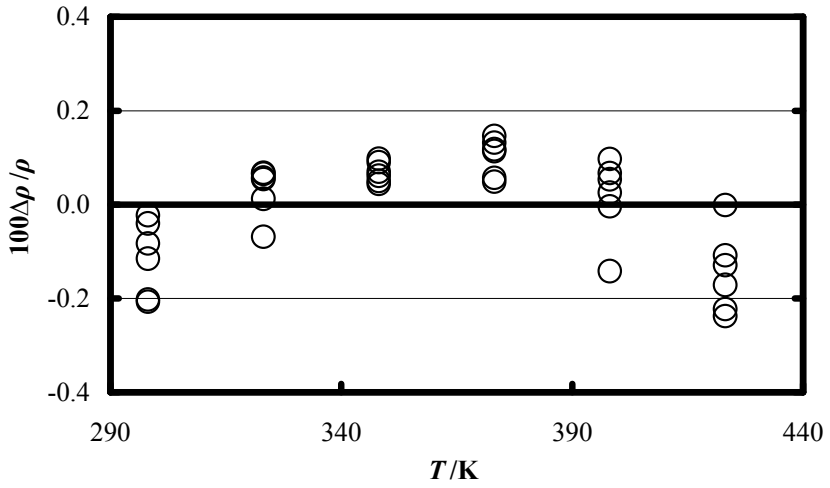

Figure 6.1. Fractional deviations $\Delta\rho/\rho = \{\rho - \rho(\text{calc})\}/\rho(\text{calc})$ of the experimentally determined density ρ of the DIDP of Table 6.2 for sample B with $w(\text{B}) = 417 \cdot 10^{-6}$ from the value obtained from eq 1.5, $\rho(\text{calc})$ as a function of T.

Another vibrating tube densimeter (DMA 602 H) was utilized for obtaining density measurements of samples A, B and C with different water contents. Prior to performing the measurements on these samples, the densimeter was calibrated with vacuum and water[31] and then the calibration parameters of the densimeter were validated with measurements on toluene[32] and octane[17]. The experimental density data obtained of these samples are listed in Table 6.3 with an anticipated uncertainty of 0.1 %.

Table 6.3: Experimental densities ρ_r of the samples A, B and C of diisodecyl phthalate with water mass fraction w obtained with a vibrating tube densimeter (DMA 602 H) at temperatures T and p = 0.1 MPa.

Sample	$10^6 \cdot w$	T/K	ρ_r/kg·m^{-3}	T/K	ρ_r/kg·m^{-3}
A	20	298.15	963.66	348.15	927.67
		323.15	945.62	363.15	916.97
A	115	298.15	963.63	348.15	927.66
		323.15	945.55	363.15	916.89
B	24	298.15	963.85	348.15	927.74
		323.15	945.66	363.15	917.07
B	417	298.15	963.81	348.15	927.68
		323.15	945.64	363.15	916.95
C	29	298.15	964.61	348.15	928.23
		323.15	946.14	363.15	917.53
C	236	298.15	964.99	348.15	928.51
		323.15	946.41	363.15	917.80

Figure 6.2 shows the fractional deviations of the experimental densities given in Table 6.3 from these calculated from eq. 1.6 where the adjustable parameters were determined by a least square fit with a standard deviation of 0.04 % and found to be A_0 = 1201.056, A_1 = -0.856 and A_2= $2.04 \cdot 10^{-4}$ where all values lie within the expanded uncertainty of ±0.1%.

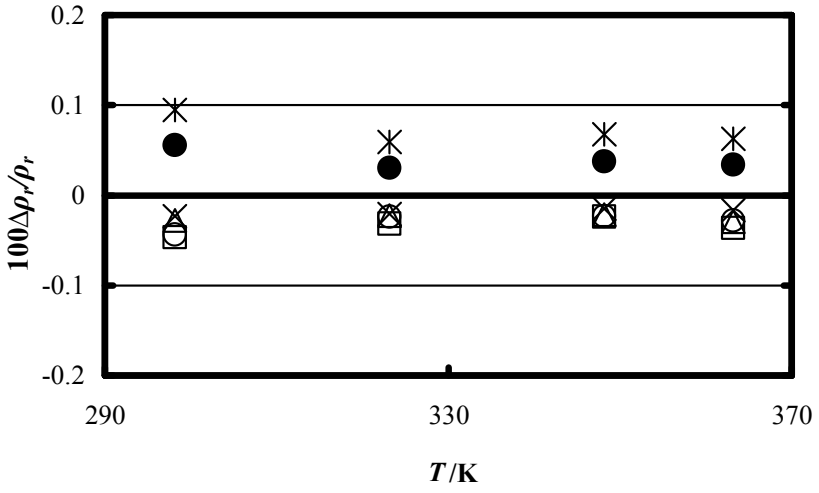

Figure 6.2. Fractional deviations $\Delta\rho_r/\rho_r = \{\rho_r - \rho_r(\text{calc})\}/\rho_r(\text{calc})$ of the experimentally determined density ρ_r of the DIDP of Table 6.3 from the value obtained from eq 1.5. at p = 0.1 MPa as a function of temperature T . □, sample A with A(w) = $115 \cdot 10^{-6}$; ○, sample A with A(w) = $20 \cdot 10^{-6}$; ∗, sample C with C(w) = $236 \cdot 10^{-6}$; ●, sample C with C(w) = $29 \cdot 10^{-6}$; ×, sample B with B(w)= 24 10^{-6}; △, sample B with B(w)= $417 \cdot 10^{-6}$.

6.2 Results for viscosity:

The experimental measurements of viscosity of sample B of $w = 417 \cdot 10^{-6}$, sample A of $w = 20 \cdot 10^{-6}$ and sample C of $w = 29 \cdot 10^{-6}$ at $p = 0.1$ MPa are presented in Table 6.4. These measurements were correlated by the Vogel equation, eq. 1.4, with a standard deviation of $\pm$ 0.15 % and the parameters obtained by a non-linear regression are $e = -2.6164$, $f = 787.0715$ and $g = -187.1792$.

Table 6.4 Experimental viscosities of sample B, sample A and sample C with water mass fraction w at temperature T and $p = 0.1$ MPa.

Sample	$10^6 \cdot w$	T/K	η_0/mPa·s
B	417	298.15	87.50
		303.15	64.60
		308.15	48.99
		313.15	37.74
		323.15	23.85
		348.15	9.72
		373.15	5.03

Table 6.4 continued

Sample	$10^6 \cdot w$	T/K	η_0/mPa·s
		398.15	3.04
		423.15	2.05
A	20	298.15	87.2
		323.15	23.85
		348.15	9.71
		363.15	6.39
B	29	298.15	87.3
		323.15	23.84
		348.15	9.71
		363.15	6.39

Viscosity results at $p > 0.1$ MPa for sample B with $w(\mathrm{B}) = 4.17 \cdot 10^{-6}$ are tabulated in Table 6.5 and were fitted to the empirical Vogel-Fulcher–Tammann function (VFT), eq. 1.8, with a standard deviation of 1%. The obtained coefficients are presented in Table 6.6.

Table 6.5 Experimental viscosities η determined with a vibrating wire viscometer for sample B with water mass fraction $w = 4.17 \cdot 10^{-6}$ at temperature T and pressure p >0.1 MPa.

T/K	*p*/MPa	η/mPa·s	*T*/K	*p*/MPa	η/mPa·s
298.15	10	107.34	323.15	10	29.24
303.15	10	78.53	323.15	20	35.63
303.15	20	98.01	323.15	30	42.46
303.15	30	120.88	323.15	50	60.41
308.15	10	60.34	323.15	70	80.63
308.15	20	73.13	348.15	10	11.55
308.15	30	89.03	348.15	20	13.81
308.15	50	135.40	348.15	30	15.93
313.15	10	46.50	348.15	50	21.50
313.15	20	57.00	348.15	70	28.86
313.15	30	68.14	373.15	10	5.92
313.15	50	100.07	373.15	20	6.96

Table 6.5 continued

T/K	*p*/MPa	η/mPa·s	*T*/K	*p*/MPa	η/mPa·s
373.15	30	7.84	398.15	70	7.64
373.15	50	10.33	423.15	10	2.40
373.15	70	13.45	423.15	20	2.71
398.15	10	3.60	423.15	30	3.00
398.15	20	4.12	423.15	50	3.86
398.15	30	4.74	423.15	70	4.83
398.15	50	5.98			

Table 6.6. Coefficients of eq. 1.8 for the viscosity of sample B reported in Table 6.5 with $w(\mathrm{B})= 4.17\cdot10^{-4}$

a	*b*	*c*	*d*	*e*	T_0
-2.61259	0.00429	792.27258	2.14952	-0.00469	186.15040

Figure 6.3 shows the fractional deviations of viscosities listed in Table 6.5 for sample B with $w(\mathrm{B}) = 4.17 \cdot 10^{-4}$ from eq. 1.8 with coefficients of Table 6.6 as a function of η. All the measurements lie within the estimated expanded uncertainty of about ±2% except for $\eta(308.15\ \mathrm{K}, 50\ \mathrm{MPa}) \approx 135\ \mathrm{mPa \cdot s}$ when the difference is +2.8 %.

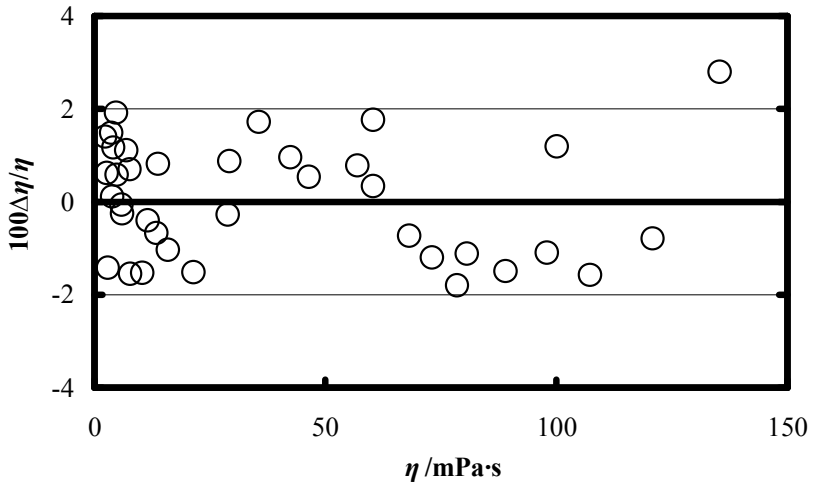

Figure 6.3 Fractional deviations $\Delta\eta/\eta = \{\eta - \eta(\mathrm{calc})\}/\eta(\mathrm{calc})$ of the experimentally determined viscosity η for sample B from the value η(calc) obtained from eq. 1.8 with coefficients of Table 6.6 as a function viscosity.

6.3 Comparison with literature data:

Viscosities and densities measurements presented in this work were compared with values reported in the literature. The densities reported by Harris *et* al.[26] and Caetano *et al*.[3,24,25] of DIDP were compared with the results obtained in this work and are shown in Figure 6.4 as a deviation from values ρ(calcd) calculated from eq. 1.5 with coefficients obtained from the values listed in Table 6.3. Although the literature values are systematically below those obtained in this work they agree within the mutual uncertainties.

The viscosities of DIDP obtained using vibrating wire of nominal diameter of 0.15 mm were also compared with values reported in the literature obtained by a vibrating viscometer [3,24,25] and a falling body viscometer [26] with different water content *w*, in the temperature range that overlaps the range considered in this work. This comparison is illustrated as fractional deviations and is shown in Figure 6.5.

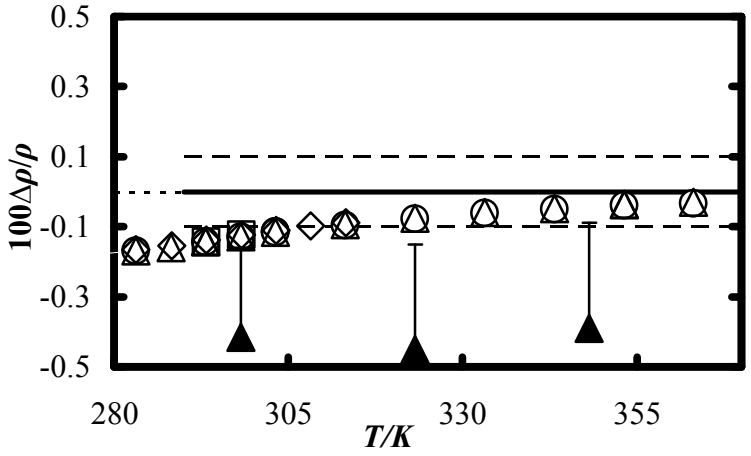

Figure 6.4 Fractional deviations $\Delta\rho/\rho = \{\rho - \rho(\text{calcd})\}/\rho(\text{calcd})$ of the experimental density ρ for DIDP from ρ(calcd) of eq. 1.5 at $p = 0.1$ MPa with the coefficients obtained from the results listed in Table 6.3 as a function of temperature T. ▲, This work sample B with $w(\text{B}) = 417 \cdot 10^{-6}$ obtained with the DMA 512 P; ◇, Caetano et al.[24] sample with purity of 0.995 and $w = 20 \cdot 10^{-6}$; □, Caetano et al.[25] sample with purity of 0.998 and $w = 107 \cdot 10^{-6}$; ○, Harris and Bair[26] sample A with purity of 0.99 dried over 0.3 nm molecular sieve with unspecified w; △, Harris and Bair[26] sample B with purity of 0.998 dried over 0.3 nm molecular sieve with unspecified w. The dashed lines at $y = \pm 0.1$ are the expanded uncertainties in the present work measurements obtained with the DMA 602 H while that at $y = 0$ indicates an extrapolation of eq. 1.5 to temperatures below the measurement range of this work.

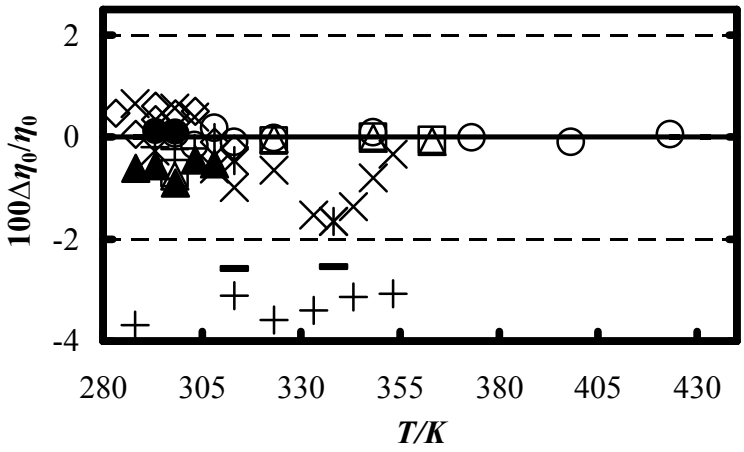

Figure 6.5 Fractional deviations $\Delta\eta_0/\eta_0 = \{\eta_0 - \eta_0\,(\text{calc})\}/\ \eta_0\,(\text{calc})$ of the experimentally determined viscosity η_0 at $p = 0.1$ MPa for different impurities and water mass fraction w, from the value obtained from eq. 1.4 η_0(calc) as a function of temperature T. △, This work, sample A with $w(\text{A}) = 20\cdot10^{-6}$; ○, this work sample B with $w(\text{B}) = 417\cdot10^{-6}$; □, this work sample C with $w(\text{C}) = 29\cdot10^{-6}$; ▲, Caetano *et al*.[3] with purity of 0.995 and $w = 20\cdot10^{-6}$; ◇, Caetano *et al*.[24] with purity of 0.998 with $w = 20\cdot10^{-6}$; ●, Caetano *et al*[25] with purity of 0.998 and $w = 107\cdot10^{-6}$; ＋, Harris and Bair[26] sample of A with unspecified w obtained with Canberra viscometer; ×, Harris and Bair[26] sample of purity 0.998 and unspecified w obtained with Canberra viscometer; ∗, Harris and Bair[26] sample B with unspecified w obtained with Atlanta alpha viscometer; –, Harris and Bair[26] obtained sample C with unspecified w obtained with Atlanta alpha viscometer. The dashed lines are the expanded uncertainties in this work.

The only viscosity measurements of DIDP as a function of pressure reported in the literature at $p > 0.1$ MPa, that the author is aware of, are those conducted by Harris and Bair[26]. In the overlapping temperature and pressure range, shown in Figure 6.6, their data differ systematically from eq. 1.8 from -9 % to +11 % with increasing viscosity. Harris and Bair[26] observed differences in the viscosity of DIDP, obtained with falling body viscometers, from samples with purities of 0.99 and 0.998 that increased with increasing pressure. They speculated these differences might have arisen from variations in the isomeric composition of DIDP.

The viscosity reported for S20 sourced from different lots and suppliers varies by about ±5 %[22,30,33]. S20 is a mixture of unspecified hydrocarbons and the exact constituents and composition are proprietary, and presumably differs from lot to lot and from supplier to supplier; this fluid is required to have a nominal viscosity at $T = 298$ K and $p = 0.1$ MPa of 29 mPa·s and a specified temperature dependence within the cited uncertainty of the certified values. The plausible variations in chemical composition could also give rise to the observed variations in viscosity.

Nevertheless, DIDP can serve as an adequate calibrant of instruments intended to measure the viscosity at $p = 0.1$ MPa with an uncertainty of about ±2 % and for $p > 0.1$ MPa within about ±10 %; these uncertainty statements are equivalent to those reported for S20.

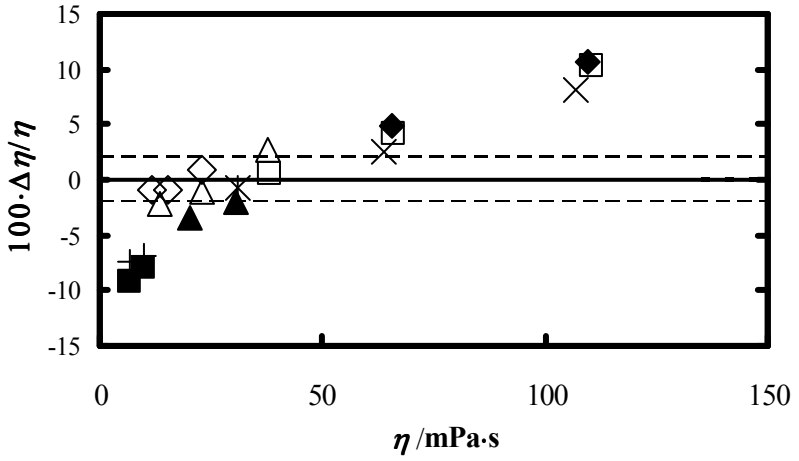

Figure 6.6. Relative deviations $\Delta\eta/\eta = \{\eta - \eta(\text{calcd})\}/\eta(\text{calcd})$ of the experimentally determined viscosity η from the value η(calcd) obtained from eq. 1.8 with coefficients of Table 6.6 as a function viscosity η. □, Harris and Bair[26] sample B Canberra viscometer at $T = 313$ K; △, Harris and Bair[26] sample B Canberra viscometer at $T = 338$ K; ◊, Harris and Bair[26] sample B Canberra viscometer at $T = 348$ K; ◆, Harris and Bair[26] sample B Atlanta alpha viscometer at $T = 313$ K; ▲, Harris and Bair[26] sample B Atlanta alpha viscometer at $T = 338$ K; ■, Harris and Bair[26] sample B Atlanta alpha viscometer at $T = 373$ K; ×, Harris and Bair[26] sample C Atlanta alpha viscometer at $T = 338$ K; ∗, Harris and Bair[26] sample B Atlanta alpha viscometer at $T = 338$ K; +, Harris and Bair[26] sample C Atlanta alpha viscometer at $T = 373$ K. The dashed lines are the expanded uncertainties in this work measurement.

Chapter 7

SOLUBILITY MEASUREMENT

7.1 Introduction:

This work, in addition to measurements on DIDP, involves the design and the initial testing of an apparatus for simultaneously measuring the solubility of a gas in a high molecular weight liquid hydrocarbon, typical of a heavy oil and the viscosity and density of the resulting gas + oil mixture over a wide temperature and pressure range.

7.2 Aim and definition:

The production of heavy viscous petroleum fluid from the well can be enhanced by dissolving gas, which will reduce its viscosity and consequently increase the production rate. The maximum gas amount that can be dissolved in a liquid at a certain temperature and pressure is expressed by the solubility x[34]. Quantitatively, it can be defined as the mole fraction of the dissolved gas in the liquid, i.e.

$$x = \frac{n_{dg}}{n_{dg} + n_l} \qquad (1.7)$$

where n_g and n_l are number of moles of the absorbed gas and the liquid respectively. The calculation procedure of obtaining n_{dg} and n_l is discussed in more detail in the subchapter 7.4, where the

solubility can be obtained from very high precision measurements of the change in pressure of the gas above the solution during the dissolution process.

7.3 Experimental setup:

Figure 7.1 shows a schematic diagram of the solubility apparatus. It consists of a vibrating wire viscometer of a nominal diameter of (0.4) mm, thicker than that which was used for measuring the DIDP viscosity; a vibrating tube densimeter (Anto Paar DMA, model 512 P), a pressure transducer (Paroscientific™ model 1001-1k-06); an accumulator vessel; a magnetic pump and a thermostatic bath. A cylindrical pressure vessel was used to accommodate the vibrating wire and the liquid, was fabricated from non-magnetic stainless steel grade 316.

The theory of the viscometer requires previous knowledge of the wire radius R and the internal damping factor $\triangle_0$. The radius was precisely determined by employing a calibration procedure where water was used as a calibrating fluid then the result was validated with toluene. The wire radius was found to be 0.184 mm. The internal damping factor $\triangle_0$ was determined from the measurement of the resonance curve in vacuum and was $200 \cdot 10^{-6}$.

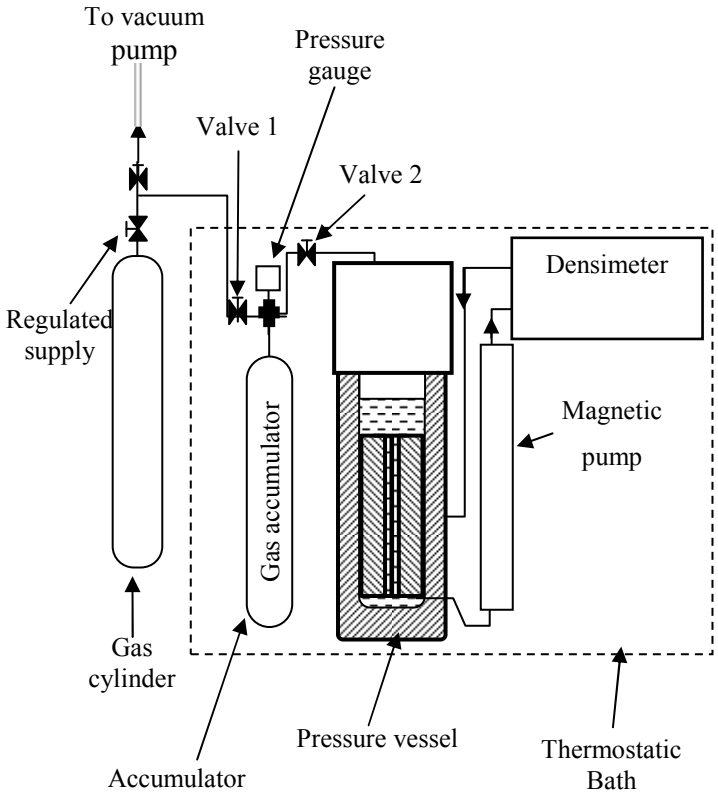

Figure: 7.1 gas solubility apparatus

Figure 7.2 shows a diagrammatic cross-section of the magnetically activated mixing pump which was used to mix the fluid. It consists of a cylinder, a fitted piston, a check-valve and magnet rings. The piston was fabricated from 420 series magnetic stainless steel and was magnetically caused to move by samarium-cobalt magnet rings which were placed outside the cylinder. The cylinder was constructed from grade 316 stainless steel. The check-valve was

mounted at the top the piston which was made of a thin circular of stainless steel grade 316. At the bottom of the piston a ball of PTFE was used to work as a non-return valve. The magnet rings were moved up and down manually during the initial test and a variable speed electric motor will be used in the future.

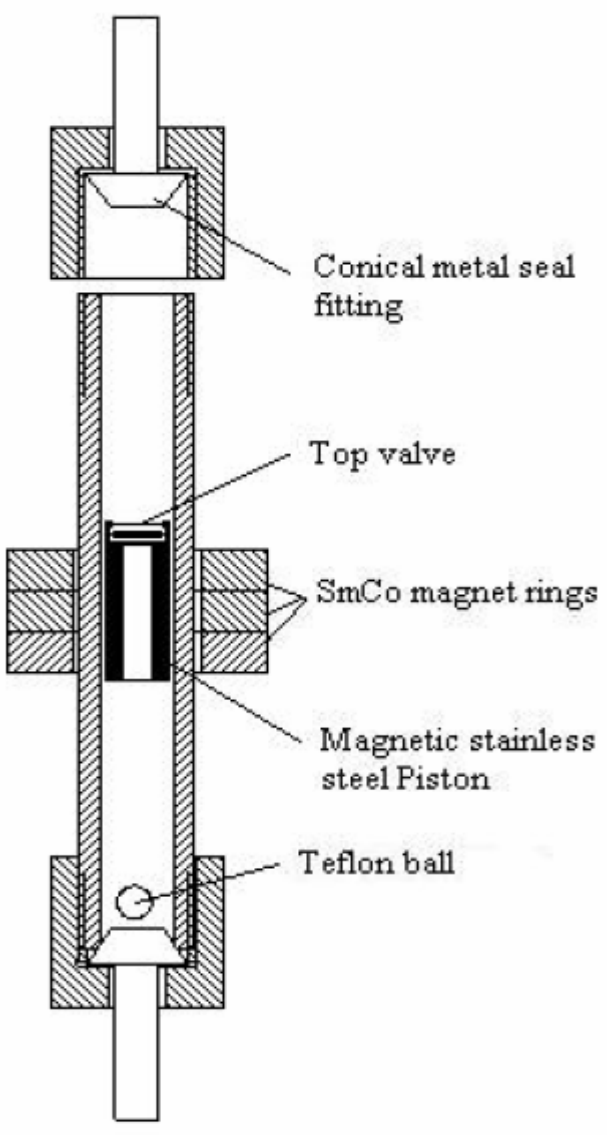

Figure: 7.2 diagrammatic cross-section of the magnetic pump.[4]

7.4 Calculation procedure

The measurement of the solubility was made on the system of squalane (highly branched C_{30} alkane) + carbon dioxide as an initial test of the apparatus operation. Squalane (2,6,10,15,19,23-hexamethyl tetracosane, $C_{30}H_{62}$) has a molecular structure shown in Figure 7.3, and was purchased from Aldrich with a batch number of 07729CE and a mass fraction purity stated to be greater than 99 %.

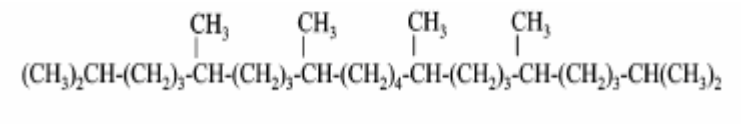

Figure 7.3 molecular structure of squalane.

The sample was dried over activated grade 0.4 nm molecular sieves prior to use. GLC with FID and chrompack capillary column indicated the mass fraction > 0.9970. The column temperature was 250 ^{o}C while the FID and the injector temperature was 350 ^{o}C and 300 ^{o}C respectively. The mass fraction of water in the sample was determined by a Karl Fisher titration using Radiometer Analytical, TIM 550 and found to be at $5 \cdot 10^{-6}$.

In order for the number of moles of absorbed gas, n_{dg}, and thus the solubility x to be calculated the apparatus was divided into two volumes as shown in figure 7.4. The first volume v_1 is the accumulator and the volume of the connecting and tubing between valve 1 and valve 2, while the second volume v_2 is the volume above the liquid in the pressure vessel and the additional volume of the tube that connects the pressure vessel to valve 2. Typically, v_1 was 150.72 cm^3 and v_2 was 37.62 cm^3. By considering this division, expansion measurements can be made and hence the solubility of a gas can then be evaluated from the saturated pressure after the gas expanded. The number of moles of the absorbed gas can be calculated by subtracting the initial number of moles of gas in v_1 from the number of moles of gas in the combined volumes, v_1 plus v_2, at the saturation pressure p_{sat}. The molecular weight of squalane was taken to be 422.83 g/mol which was used to obtain the number of moles of squalane sample. The inner diameter of the pressure vessel was 38.5 mm and was 40 mm high.

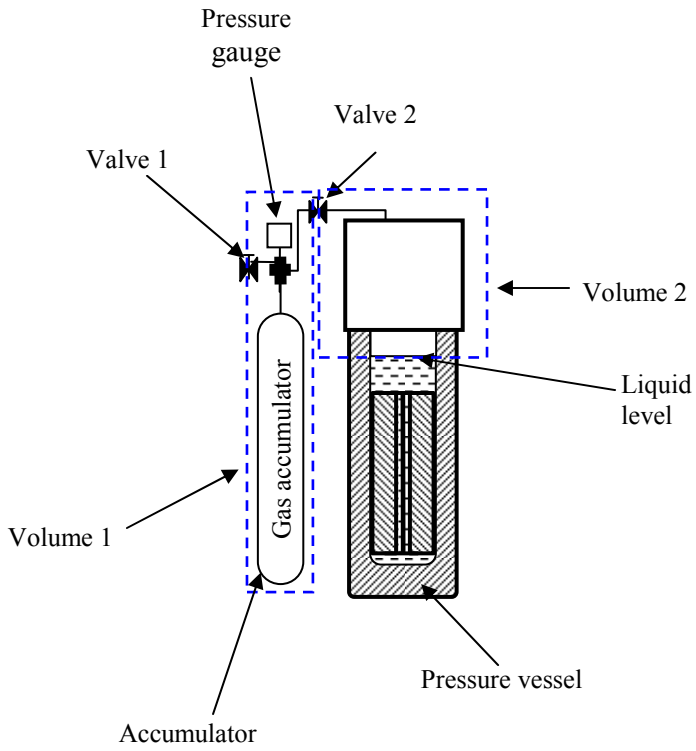

Figure: 7.4 Sketch illustrating the defined volumes (1 and 2)

The exact procedure was carried out as follows: (a) a known amount of the squalane was placed in the vessel; (b) the entire apparatus was evacuated; (c) valve 2 was closed and the volume 2 was filled slowly with carbon dioxide until a desired pressure was reached p_1; (d) the gas was expanded into volume v_2 by opining valve 2 and when the total pressure in the two volumes was at equilibrium the total number of moles of the gas in the combined volume, after expansion but before absorption, was determined from equation 7.2; (e) then the two phases were mixed by using the

magnetic pump until an equilibrium saturation pressure was reached; (f) the number of moles of residual gas was determined from equation 7.3; (g) the number of dissolved gas was calculated by subtracting equation 7.3 from equation 7.2.

The number of moles of gas in combined volume, n_1 and n_2, after expansion but before absorption is

$$n_1 + n_2 = \frac{p_t(v_1 + v_2)}{RT} \qquad (7.2)$$

where T is the desired temperature in Kelvin and R is the gas constant (8.31447 MPa·cm^3·mol^{-1}·K^{-1}).

The number of moles of gas at the saturation pressure is

$$n_1 + n_2 - n_{dg} = \frac{p_{sat}(v_1 + v_2)}{RT} \qquad (7.3)$$

The number of moles of dissolved gas was calculated by subtracting equation 7.3 from 7.2, yielding

$$n_{dg} = \frac{(v_1 + v_2)\cdot(p_t - p_{sat})}{RT} \qquad (7.4)$$

The equation was used under the assumption that the vapour pressure squalane at 293.15 K was negligible, typically 0.000266 MPa at 513.15 K as stated by the supplier.

7.5 Preliminary results

A sample of squalane, typically 20 g, was placed in the pressure vessel. After that, the entire system was evacuated and volume one, v_1= 150.72 cm^3, was filled with carbon dioxide until the pressure reached 20.05 bar. Pressure expansion was made from volume one into volume two and the two phases, the liquid and the gas, were mixed well until the pressure was stable at 3.0478 bar. The density and viscosity of the resulting mixture and the solubility of carbon dioxide were all measured at 293.15 K and at 3.0478 bar. The calculated solubility x was 0.0081. The density and viscosity of the resulting mixture were 808.37 $kg \cdot m^{-3}$ and 23 mPa·s respectively.

Bibliography

1. Künzel, W.; Van Wijk, H. F.; Marsh, K. N., *Viscosity. In Recommended reference materials for the realization of physicochemical properties*. Blackwells: Oxford,U.K., 1987; p 45-72.

2. Dymond, J. H.; Oye, H. A., Viscosity of selected liquid n-alkanes. *J. Phys. Chem. Ref. Data* **1994,** 23, 41-53.

3. Caetano, F. J. P.; Fareleira, J. M. N. A.; Oliveira, C. M. B. P.; Wakeham, W. A., Viscosity of Di-isodecylphthalate: A Potential Standard of Moderate Viscosity. *International Journal of Thermophysics* **2004,** 25, 1311-1322.

4. Kandil, M. E. The Development of A Vibrating Wire Viscometer and A Microwave Cavity Resonator. Ph.D. Thesis, University of Canterbury, Christchurch, 2005.

5. Kandil, M. E.; Marsh, K. N.; Goodwin, A. R. H., Vibrating Wire Viscometer with Wire Diameters of (0.05 and 0.15) mm: Results for Methylbenzene and Two Fluids with Nominal Viscosities at T = 298 K and p = 0.01 MPa of (14 and 232) mPa.s at Temperatures between (298 and 373) K and Pressures below 40 MPa. *Journal of Chemical and Engineering Data* **2005,** 50, 647-655.

6. Douglas, J. F.; Gasiorek, J. M.; Swaffield, J. A., *Fluid mechanics*. 4th ed.; Prentice Hall: Upper Saddle River, NJ, 2001; p 6-13,100-102.

7. Nagala, D. W.; Boufaida, M., The importance of online viscosity measurement for leak detection and other simulation applications. In *International Pipeline Conferece*, Calgary, Alberta, Canada, 2004.

8. Van Wazer, J. R.; Lyons, J. W.; Kim, K. Y.; Colwell, R. E., *Viscosity and flow measurement : a laboratory handbook of rheology*. Interscience Publishers: New York, 1963; p 406.

9. Wakeham, W. A.; Nagashima, A.; Sengers, J. V., *Measurement of theTransport Properties of Fluids*. Blackwell Scientific Publications for IUPAC: Oxford U.K. , 1991; p 8-110.

10. Dinsdale, A.; Moore, F., *Viscosity and its measurement*. Chapman and Hall: London, 1962; p 1-60.

11. Alexander, A. E.; Anderson, J. R.; Arthur, J. C.; Bauer, N.; Beyer, G. L.; Corwin, A. H.; Harkins, W. D.; Lewin, S. Z.; Mader, W. J.; Mark, H.; Moore, L. D.; Simonsen, D. R.; Skau, E. L.; Sturtevant, J. M., *Physical methods of organic chemistry*. 1 st. ed.; Interscience Publishers: New York, 1959; Vol. I, p 12.

12. Daniels, F.; Williams, J. W.; Bender, P.; Alberty, R. A.; Cornwell, C. D.; Harriman, J. E., *Experimental physical chemistry*. 7th . ed.; McGraw-Hill: New York, 1970; p 157-163.

13. Reid, R. C.; Prausnitz, J. M.; Poling, B. E., *The properties of gases and liquids*. 4th . ed.; McGraw-Hill: New York, 1987; p 388-470.

14. Vogel, H., The law of the relation between the viscosity of liquids and the temperature. *Phys. Z.* **1921,** 22, 645-646.

15. Scherer, G. W., Editorial comments on a paper by Gordon S. Fulcher. *J.Am. Ceram Soc.,* **1992,** 75, 1060-1062.

16. Hayward, A. T. J., Compressibility equations for liquids: a comparative study. . *Br. J. Appl. Phys.* **1967,** 18, 965-977.

17. Caudwell, D. R. Viscosity of Dense Fluid Mixtures. Ph.D. Thesis, Imperial College, London, 2004.

18. Swindells, J. F.; Coe, J. R.; Godfrey, T. B., Absolute Viscosity of Water at 20 ^{0}C. . *J. Res. Natl. Bur. Stand. (U.S.)* **1952,** 48, 1-31.

19. R. Mostert; P.S. Van Der Gulik; H.R. Van Den Berg, The working equations of a vibrating wire viscometer. *Physica A* **1989,** 156, 909-920.

20. Retsina, T.; Richardson, S. M.; Wakeham, W. A., The theory of a vibrating-rod viscometer. *Applied Scientific Research* **1987,** 43, 325-346.

21. Retsina, T.; Richardson, S. M.; Wakeham, W. A., The theory of a vibrating-rod densimeter. *Applied Scientific Research* **1986,** 43, 127-158.

22. Kandil, M. E.; Harris, K. R.; Goodwin, A. R. H.; Hsu, K.; Marsh, K. N., Measurement of the Viscosity and Density of a Reference Fluid, with Nominal Viscosity at T = 298 K and p = 0.1 MPa of 29 mPa.s, at Temperatures between (273 and 423) K and Pressures below 275 MPa. *Journal of Chemical & Engineering Data* **2006,** 51, 2185-2196.

23. Padua, A. A. H.; Fareleira, J. M. N. A.; Calado, J. C. G.; Wakeham, W. A., Electromechanical model for vibrating-wire instruments. *Review of Scientific Instruments* **1998,** 69, 2392-2399.

24. Caetano, F. J. P.; Fareleira, J. M. N. A.; Oliveira, C. M. B. P.; Wakeham, W. A., New Measurements of the Viscosity of Diisodecyl Phthalate Using a Vibrating Wire Technique. *Journal of Chemical and Engineering Data* **2005,** 50, 1875-1878.

25. Caetano, F. J. P.; Fareleira, J. M. N. A.; Fernandes, A. C.; Oliveira, C. M. B. P.; Serro, A. P.; Simões de Almeida, I. M.; Wakeham, W. A., Diisodecylphthalate (DIDP)-a potential standard of moderate viscosity: Surface tension measurements and water content effect on viscosity. *Fluid Phase Equilibria* **2006,** 245, 1-5.

26. Harris, K. R.; Bair, S., Temperature and Pressure Dependence of the Viscosity of Diisodecyl Phthalate at Temperatures Between (0 and 100) ^{0}C and at Pressures to 1 GPa. *J. Chem. Eng. Data ASAP 10.1021/je060382+* **2006**.

27. Tough, J. T.; McCormick, W. D.; Dash, J. G., Viscosity of liquid He II. *Physical Review* **1963,** 132, 2373-8.

28. Assael, M. J.; Papadaki, M.; Dix, M.; Richardson, S. M.; Wakeham, W. A., An absolute vibrating-wire viscometer for liquids at high pressures. *International Journal of Thermophysics* **1991,** 12, 231-44.

29. Assael, M. J.; Oliveira, C. P.; Papadaki, M.; Wakeham, W. A., Vibrating-wire viscometers for liquids at high pressures. *International Journal of Thermophysics* **1992,** 13, 593-615.

30. Lundstrum, R.; Goodwin, A. R. H.; Hsu, K.; Frels, M.; Caudwell, D. R.; Trusler, J. P. M.; Marsh, K. N., Measurement of the Viscosity and Density of Two Reference Fluids, with nominal Viscosities at T = 298 K and p = 0.1 MPa of (16 and 29) mPa.s, at Temperatures between (298 and 393) K and Pressures below 55 MPa. *Journal of Chemical and Engineering Data* **2005,** 50, 1377-1388.

31. Wagner, W.; Pruss, A., The IAPWS Formulation 1995 for the Thermodynamic Properties of Ordaniary Water Substance for General and Scientific Use. *J. Phys. Chem. Ref. Data* **2002,** 31, 387-535.

32. Assael, M. J.; Avelino, H. M. T.; Dalaouti, N. K.; Fareleira, J. M. N. A.; Harris, K. R., Reference Correlation for the Viscosity of Liquid Toluene from 213 to 373 K at pressures to 250 MPa. *Int. J. Thermophys.* **2001,** 22, 789-799.

33. Sopkow, T.; Goodwin, A. R. H.; Hsu, K., Vibrating Wire Viscometer with Nominal Wire Diameter of 0.15 mm: Measurement of the Viscosity of Two Certified Reference Fluids, with Nominal Viscosities at T = 298 K and p = 0.1 MPa of (16 and 29) mPa.s, at Temperatures between (298 and 353) K and Pressures below 55 MPa. *Journal of Chemical and Engineering Data* **2005,** 50, 1732-1735.

34. Le Neindre, B.; Vodar, B., *Experimental thermodynamics*. Butterworth;: London, 1973; Vol. II, p 725-740.